Antonio Luna · Joan C. Vilanova
Pablo R. Ros *Editors*

Learning Abdominal Imaging

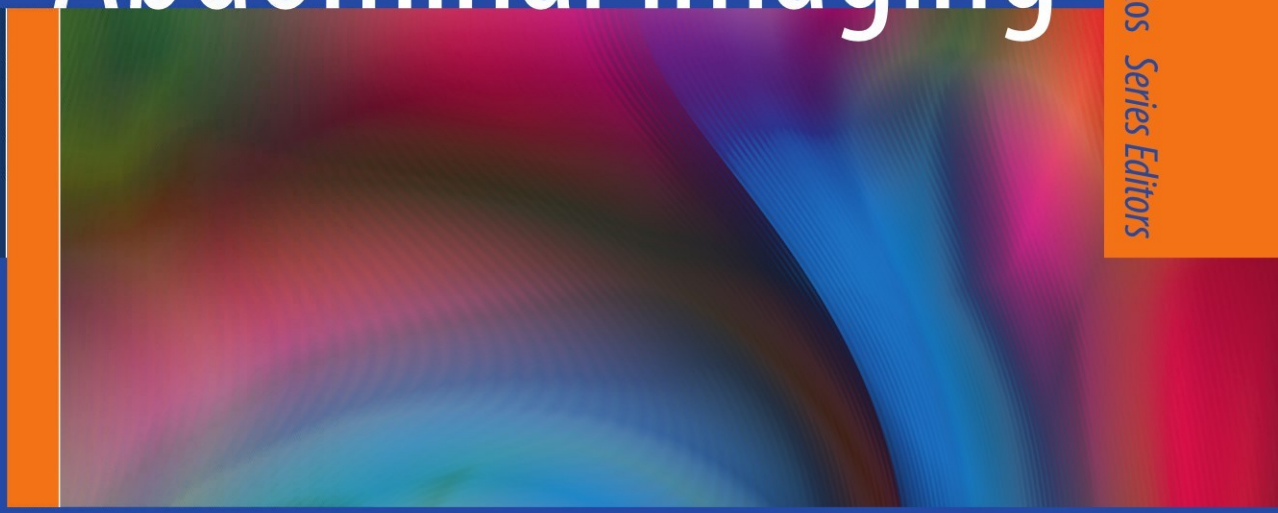

LEARNING IMAGING
Ramón Ribes · Antonio Luna · Pablo R. Ros *Series Editors*

Springer

Learning Imaging

Series Editors:

R. Ribes · A. Luna · P.R. Ros

Antonio Luna · Joan C. Vilanova
Pablo R. Ros
(Editors)

Learning Abdominal Imaging

Springer

Antonio Luna
Clinica Las Nieves Sercosa
Carmelo Torres 2
23007 Jaén
Spain

Joan C. Vilanova
Clinica Girona
Dept. Magnetic Resonance
Lorenzana 36
17002 Gerona
Spain

Pablo R. Ros
Case Western Reserve University
Dept. Radiology
Bolwell B124
Euclid Ave. 11100
44106 Cleveland Ohio
USA

ISBN 978-3-540-88002-8 e-ISBN 978-3-540-88003-5

DOI 10.1007/978-3-540-88003-5
Springer Heidelberg Dordrecht London New York

Library of Congress Control Number: 2012931857

Printed on acid-free paper

9 8 7 6 5 4 3 2 1

Springer is part of Springer Science+Business Media (www.springer.com)

Contents

Contributors

Sandra Baleato
Department of Radiology
CHUS Complexo Hospitalario
Universitario de Santiago
Santiago de Compostela
Coruña
Spain

Joaquim Barceló
Department of Radiology
Clínica Girona-Hospital Sta. Caterina
University of Girona
Girona, Spain

Maria Boada
Magnetic Resonance
Clinica Girona
Girona
Spain

Enrique Ramón Botella
Body Section
Radiology Department
Gregorio Marañon Hospital
Madrid
Spain

Gabriel C. Fernández
Department of Radiology
HNSS (Hospital Nuestra
Señora de Sonsoles)
Avila, Spain

Guadalupe Garrido
Radiology Department
Hospital Clínico
Málaga
Spain

Antonio Luna
Health Time Group and
MRI Section
Clinica Las Nieves Sercosa
Jaén
Spain

Luis Luna
Clinica Las Nieves
Sercosa
Jaén
Spain

Carmen Villalba Martín
Department of Radiology
Complexo Hospitalario Universitario de Santiago de Compostela
Santiago de Compostela, Spain

Lidia Alcalá Mata
Clinica Las Nieves Sercosa
Jaen
Spain

Xavier Merino-Casabiel
Unitat RM, Servei Radiologia
Hospital Vall d'Hebrón
Barcelona
Spain

Joaquina Paz López Moras
Centro de Diagnostico "Dr Enrique Rossi"
Buenos Aires
Argentina

Anaberta Bermúdez Naveira
Department of Radiology
Complexo Hospitalario Universitario de Santiago de Compostela
Santiago de Compostela
Spain

Teodoro Martín Noguerol
MRI Section
Clinica Las Nieves Sercosa
Jaén
Spain

María Mercedes Liñares Paz
Department of Radiology
Complexo Hospitalario Universitario de Santiago de Compostela
Santiago de Compostela
Spain

Pablo R. Ros
Department of Radiology
University Hospitals Case Medical Center
Theodore J. Castele University
Case Western Reserve University
Cleveland, OH
USA

Verónica Patricia Rubio
Centro de Diagnostico "Dr Enrique Rossi"
Buenos Aires
Argentina

Mario Santamarina
Hospital Naval Neff
Viña del Mar
Chile

Anna Pérez de Tudela
Department of Radiology
Hospital Sta. Caterina Slat
Girona
Spain

Andrés Enrique Madrid Vallenilla
Radiology Department
Gregorio Marañon Hospital
Madrid
Spain

Joan C. Vilanova
Department of Radiology
Clínica Girona-Hospital Sta. Caterina
University of Girona
Girona
Spain

Mariano Volpacchio
Centro de Diagnostico "Dr Enrique Rossi"
Buenos Aires, Argentina
Hospital de Clínicas "José de San Martín",
Buenos Aires
Argentina

Liver

1

Andrés Enrique Madrid Vallenilla, Enrique Ramón Botella, and Antonio Luna

Contents

A. Luna et al., *Learning Abdominal Imaging*, Learning Imaging,
DOI 10.1007/978-3-540-88003-5_1,

Case 1
Hemangioma

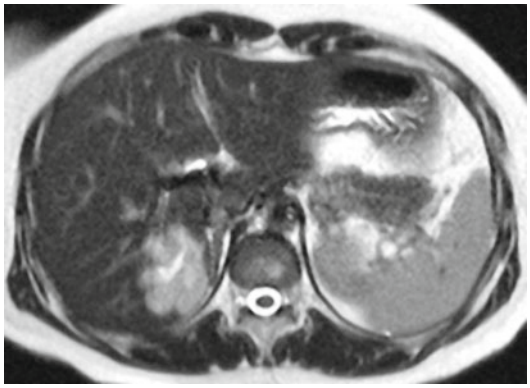

Fig. 1.1.1

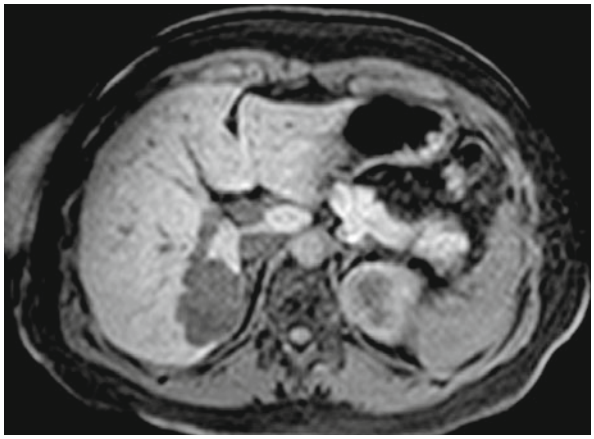

Fig. 1.1.2

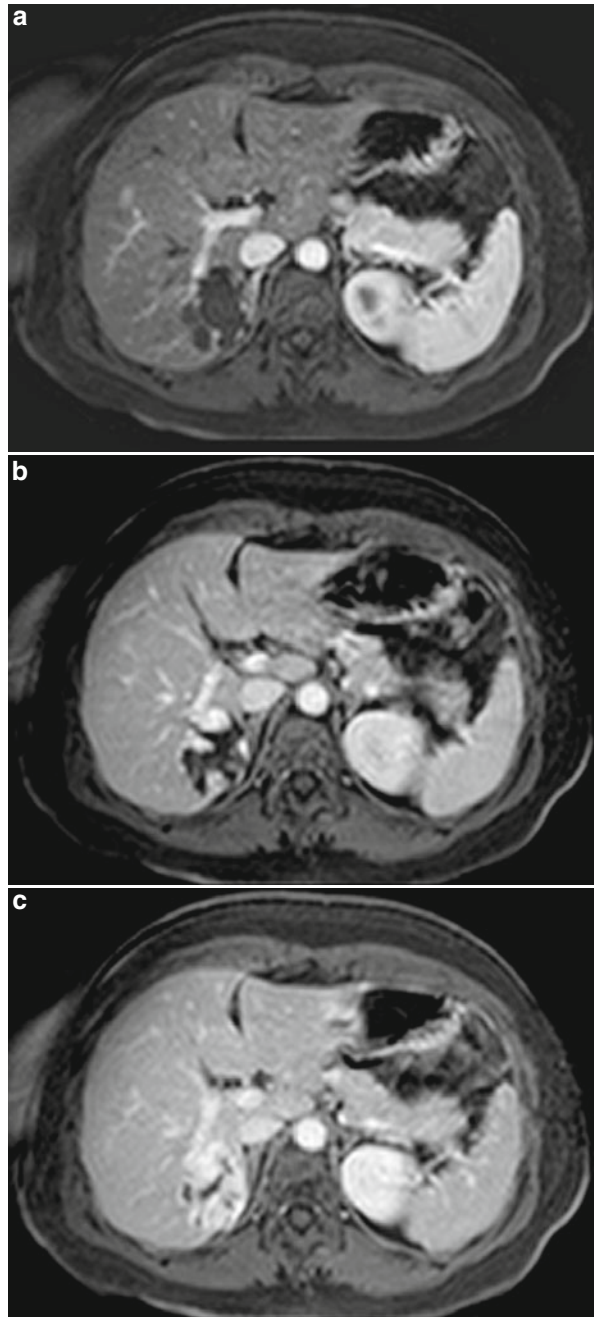

Fig. 1.1.3

A 35-year-old woman that in an abdominal ultrasound is diagnosed with a hyperechoic liver nodule in the posterior segments of the right lobe, was submitted to our MRI unit. An MRI exploration is conducted, with standard sequences, including T1-weighted, T2-weighted, and a dynamic study, after the administration of a gadolinium-based contrast media.

Comments

Hemangiomas are the most common benign tumor of the liver. Histologically they are composed of multiple vascular channels, lined by a single layer of endothelial cells, and supported by a thin fibrous stroma. They are usually detected as an incidental finding in ultrasound scans, being hyperechoic lesions with well-defined margins, which may have a slight posterior acoustic enhancement. However, sometimes, they can show atypical features. In these cases, it is crucial to perform a contrast-enhanced CT or MRI study, where they behave as hypervascular lesions, with three different possible patterns of enhancement:

Type I shows a homogeneous and rapid enhancement and tend to be small lesions.

Type II consists of a peripheral nodular enhancement with homogenous centripetal filling.

Type III is similar to type II, but there is a central scar that is not opacified with contrast; this type of enhancement is characteristic of large hemangiomas.

On T2-weighted sequences, its characteristic feature is a marked hyperintense signal, due to the high content of low-flow vascular channels. These tumors coexist very frequently with other liver lesions, and in oncologic patients with cirrhosis may cause a diagnostic problem; when the doubt exists, the T2-weighted sequence is especially useful, as it allows the radiologist to separating malignant tumor nodules from hemangiomas and cystic lesions, based on T2-relaxation differences, with an excellent diagnostic confidence.

In conclusion, the main clues to diagnose a hemangioma on MRI are the typical pattern of enhancement and its marked hyperintensity on T2.

Imaging Findings

Axial TSE T2-weighted sequence shows a focal liver lesion, measuring 4 cm in the posterior aspect of the right lobe, within the limits between segments 6 and 7 (Fig. 1.1.1). The lesion shows a lobulated shape and is markedly hyperintense, with a small central scar (*arrow*). In precontrast THRIVE (T1-weighted image), the lesion is hypointense (Fig. 1.1.2), and after contrast media injection it undergoes a peripheral nodular enhancement, with progressive centripetal filling (Fig. 1.1.3: dynamic postcontrast THRIVE series on arterial (a), venous (b), and equilibrium phases (c), respectively).

Case 2

Focal Nodular Hyperplasia

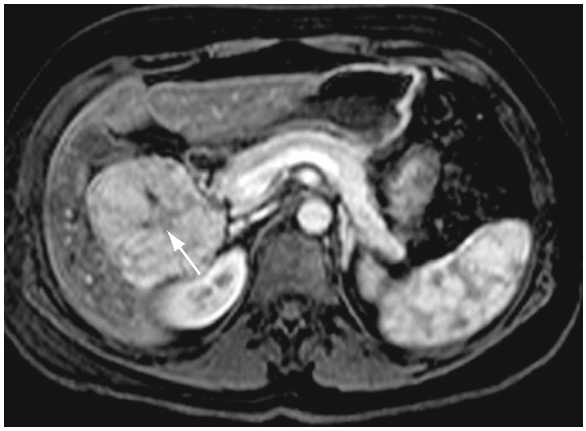

Fig. 1.2.1

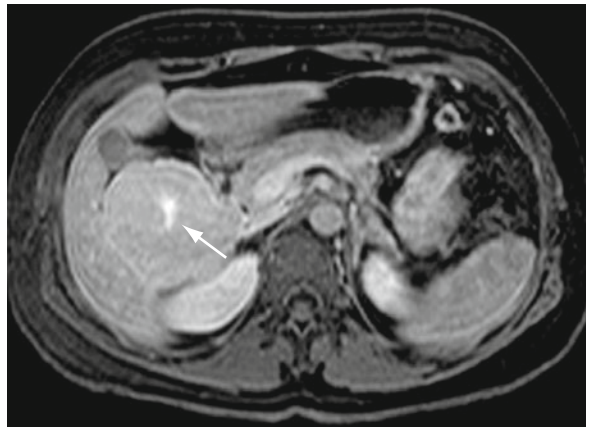

Fig. 1.2.2

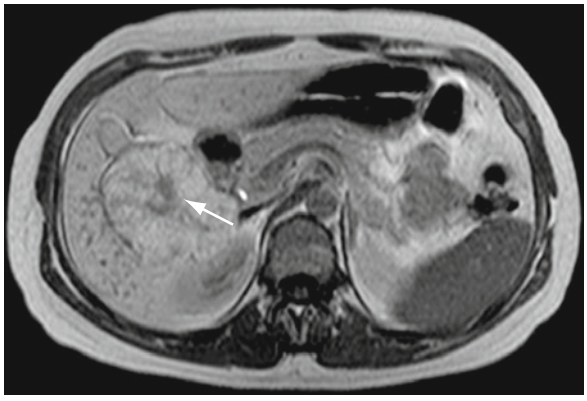

Fig. 1.2.3

A 40-year-old woman with history of epigastric pain, without any other symptom or laboratory abnormality, had an incidental finding on ultrasound of a 5-cm hepatic lesion. The lesion was subcapsular, homogeneous, and slightly hyperechoic in appearance, with a peripheral halo. An MRI was performed for further characterization.

Comments

FNH is the second most common primary solid lesion in the liver after hemangioma. It is characteristic of middle-aged women. It is usually discovered as an incidental finding. FNH is habitually a single lesion, with a homogeneous appearance in a subcapsular location. A central scar is identifiable in up to 70% of the cases, published in different series, but this finding is not pathognomonic.

In ultrasound, FNH is iso- or slightly hyperechoic compared to liver parenchyma. In Doppler or after administration of ultrasound contrast with a vascular distribution (i.e., sulfur hexachloride microbubbles), it demonstrates the characteristic pattern of centrifugal flow pattern ("spoke-wheel sign"). In dynamic CT or MRI scans, FNH shows early enhancement without washout in the equilibrium phase. The use of dual contrast at MRI allows a greater degree of diagnostic confidence. FNH is composed of functioning hepatocytes and characteristically captures the dual contrasts (Gd-BOPTA and Gd-EOB-DTPA) during biliary excretion. The dual contrasts permit to obtain a dynamic T1-weighted study, in the extracellular distribution phase, and after a variable delay between 20 and 60 min, depending on the contrast chelate used, an active intracellular transport allows to exploring the hepatocytes function, by means of their ability to secrete bile. Hepatobiliary contrast agents allow an accurate differentation between FNH and adenoma which is crucial for their management, as adenoma larger of 3 cm should be resected due to the risk of hemorrhage.

FNH as the reticuloendothelial system retains the contrasts media based on microparticles of iron (SPIO or USPIO). When this type of contrasts is used, T2-weighted sequences must be acquired, which improves the visualization of the septa and the central scar.

It has recently been marketed an ultrasound contrast that is captured by the reticuloendothelial system (perfluorobutane bubbles), and therefore it has also applicability to characterize FNH.

Imaging Findings

The lesion was isointense on both T1-weighted and T2-weighted sequences, with a central scar (images not shown). The dynamic study was performed after intravenous administration of Gd-BOPTA (gadobenate dimeglumine). The lesion showed early and intense uptake of contrast on the arterial phase with lack of enhancement of the central scar (*arrow*) (Fig. 1.2.1). During the equilibrium phase, the mass was isointense to liver parenchyma and also retains contrast at the central scar, which appeared hyperintense (*arrow*) (Fig. 1.2.2). Image in the hepatobiliary phase acquired 60 min after contrast injection shows how the mass retains contrast as much as the liver does, with lack of enhancement of the central scar (*arrow*) (Fig. 1.2.3).

Case 3
Adenoma

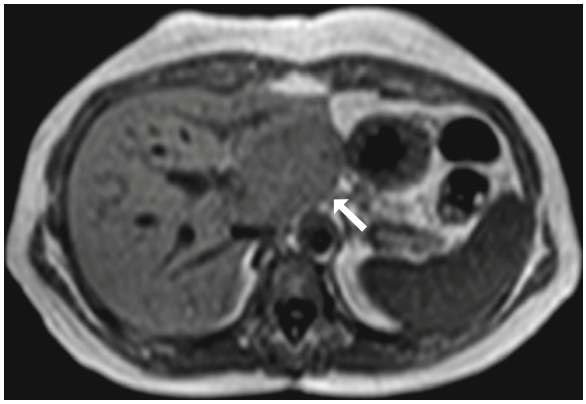

Fig. 1.3.1

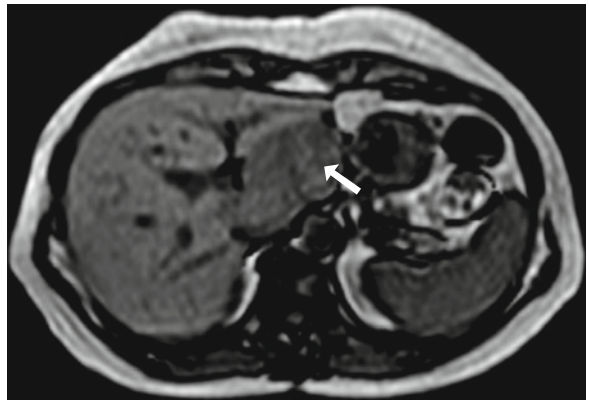

Fig. 1.3.2

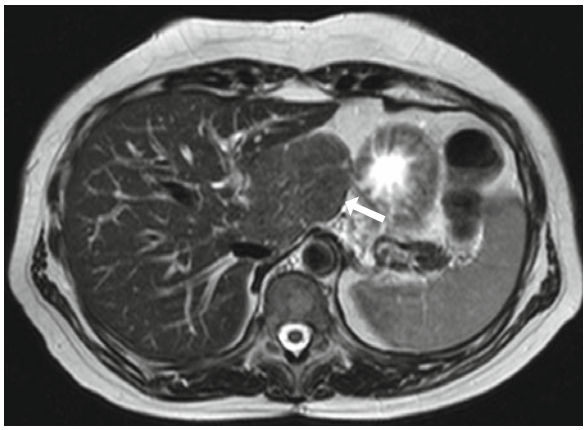

Fig. 1.3.3

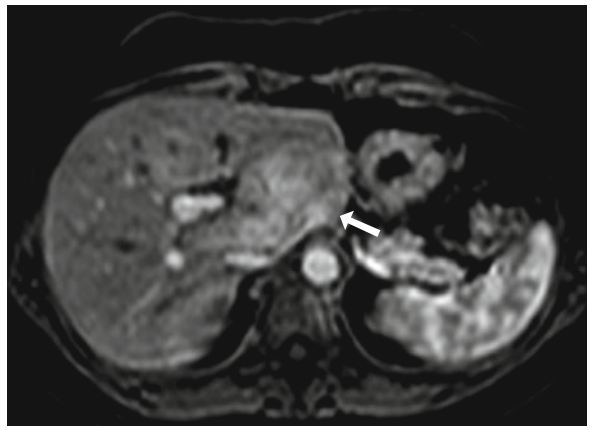

Fig. 1.3.4

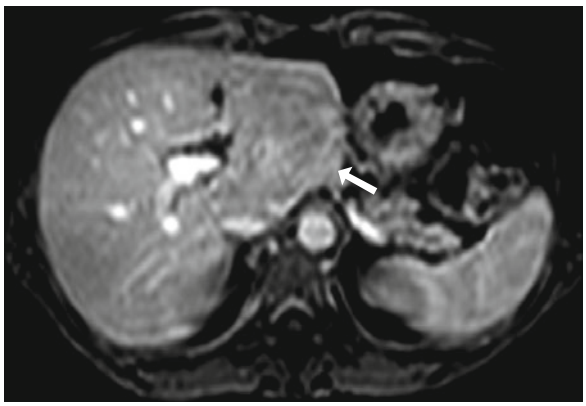

Fig. 1.3.5

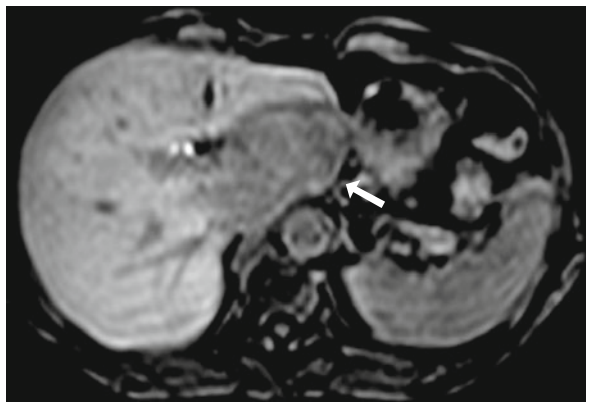

Fig. 1.3.6

A 34-year-old woman, with an incidental focal liver lesion in segment 1 on ultrasound and personal history of use of oral contraceptives, is referred to our department to perform an MRI for further characterization.

Comments

Liver adenoma is a lesion composed of hepatocytes arranged in cords. It usually has intracellular lipids and, histologically, lacks of lobules, centrilobular vein, or portal triad but shows large venous and arterial vessels in a predominant peripheral location. The presence of Kupffer cells is very rare. Large lesions may be more heterogeneous due to different components: fat, different stages of bleeding, and/or necrosis. In a considerable proportion of cases, a fibrous capsule is identifiable. The most important clinical fact is the history of oral contraceptives or anabolic steroids use.

Knowing these histological characteristics, its behavior could be predictable, in each of the imaging techniques. In US it usually correspond to hyperechogenic lesions with sharp borders. The detection of vessels is characteristic with the use of Doppler technique.

MRI is the technique of choice for characterization. The presence of fat is readily detected in GRE T1-weighted in-phase and out-of-phase images sets. The signal drop in out-of-phase with respect to in-phase images allows for the intracellular fat detection. Sometimes, adenoma may show signs of bleeding.

In the dynamic postcontrast sequence, using an extracellular contrast media, adenoma tipically shows an intense enhancement in the arterial phase, without washout in the equilibrium phase. This absence of washout helps in the distinction from hepatocellular carcinoma, which characteristically presents with washout in the equilibrium phase.

Focal nodular hyperplasia (FNH) is the main differential diagnosis of adenoma. If there is no characteristic morphological features, of either FNH, such as a scar, or adenoma, such as the presence of fat or adenoma, the distinction between both types of lesions is very challenging with both CT and MRI. However, the use of MRI dual contrasts with biliary excretion, such as dimeglumine gadobenate and gadoxetic acid, allows this distinction with a sufficient degree of diagnostic confidence. The contrast enhancement during the biliary excretion, at an intensity similar or greater than liver parenchyma, supports the diagnosis of FNH. Adenomas are characteristically hypointense compared to liver parenchyma, during the hepatospecific phase. There are between 10 to 20% of FNH with atypical features, which are classified as nonclassic. These nonclassic FNHs often present a diagnostic challenge at imaging, as they may show features typical of adenomas in different degrees.

Imaging Findings

Figure 1.3.1 In-phase GE T1 sequence confirms the presence of a slightly hypointense mass compared with liver parenchyma (*arrow*). In the out-of-phase sequence, regional signal drop within the mass is identified, revealing fat content (Fig. 1.3.2, *arrow*). In TSE T2 sequence, this lesion is isointense to liver parenchyma (Fig. 1.3.3, *arrow*). After administration of dimeglumine gadobenate, uptake in the arterial phase by the lesion is shown (Fig. 1.3.4, *arrow*). In the portal venous phase, the lesion is isointense to liver (Fig. 1.3.5, *arrow*). During the biliary excretion phase (approximately 60 min after contrast injection), the lesion does not retain the contrast, and it appears hypointense (Fig. 1.3.6, *arrow*). This enhancement pattern is typical for hepatic adenoma.

Case 4
Hepatic Lesion with Cystic Appearance: Liver Abscess

A 31-year-old woman, who came to the ER because of thoracolumbar pain, irradiating to the shoulder, and poor control with analgesics, was referred to perform an abdominal ultrasound to our department. She also refers mild malaise and was afebrile. Laboratory tests showed mild LFTs elevation and hyperbilirubinemia.

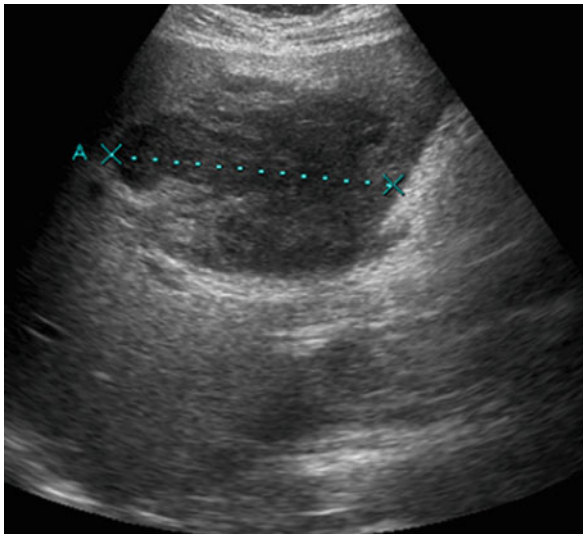

Fig. 1.4.1

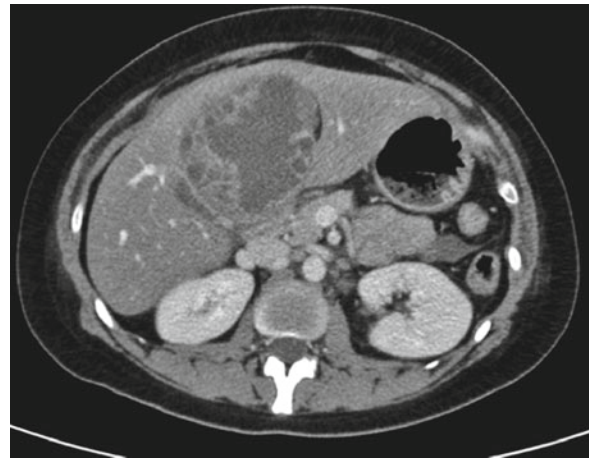

Fig. 1.4.2

Fig. 1.4.3

Comments

Liver abscesses are relatively common lesions in clinical practice and can present with very different morphology and appearance. This diagnosis must be suspected when there is a suggestive clinical scenario and a compatible liver image. They have typically a necrotic central portion with a cystic appearance, which can only be distinguished of a simple cyst because of a thick and enhancing wall. Multifocality suggests a bacterial infection, and the biliary system is the most common origin. Single lesions are more common in parasitic etiologies.

In MRI studies, abscesses may have varying intensities on T1 and T2 sequences; although often similar to a cyst, the only sign that can suggest the diagnosis is the relative restriction on DWI sequences of their content. The behavior in the dynamic study is similar to that described in CT scans.

If the clinical scenario is not supportive, other options in the differential diagnosis of the cystic lesions must be considered. Simple cysts are the most common focal lesion in the liver, usually rounded, multifocal, and lacking of an identifiable wall. The ultrasound may show septa not demonstrable with other techniques, and the typical posterior acoustic reinforcement is present. In CT scans, cysts show attenuation values between −10 and 20 HU. On MRI, cysts are markedly hyperintense on T2-weighted images and hypointense on T1-weighted sequences with lack of enhancement, on diffusion-weighted sequences, they show a similar appearance of that of the gallbladder content and should have high values on ADC maps. Cysts associated to Caroli's disease may have the "central dot" sign that corresponds to the portal triad structures, encompassed by the biliary dilatation. MRCP demonstrates communication with the bile ducts. In hepatic hydatidosis, there is usually a dominant lesion with some peripheral/satellite images. Peripheral calcification may present inside vesicles.

The group of neoplastic lesions with cystic appearance must also be taken into account. In patients above 65 years old, the cystic metastases must be considered within the diagnostic possibilities. Hepatocellular carcinoma may also present with cystic degeneration, but often preserve a solid extrinsic nodule. Biliary cystadenomas and cystadenocarcinomas are also cystic lesions. The presence of mural nodules and calcifications favors the diagnosis of malignancy.

Finally, solid tumoral lesions may undergo cystic changes when treated either by interventional techniques or chemotherapy treatments. In this setting, it can be difficult to assess the presence of tumoral tissue, MRI is particularly useful with the use of DWI and dynamic contrast enhanced sequences that helps in distinguishing necrotic degeneration from viable tumor tissue.

Imaging Findings

A lesion was identified in liver segment 4, which had irregular margins, measuring approximately 8 cm in its long axis, with heterogeneous echogenicity and mild posterior acoustic reinforcement (Fig. 1.4.1, liver ultrasound). The Doppler signal was increased in the periphery, and there was no evidence of vessels inside (not shown). The CT study identified a well-defined lesion, ovoid in shape, presenting two different components within it: a peripheral heterogeneous layer, mildly hyperdense in comparison to the surrounding liver parenchyma, and a central portion, homogeneous and with lower density (Figs. 1.4.2 and 1.4.3, enhanced CT on the portal phase and coronal MPR of enhanced CT on the portal phase). No satellite lesions or bile duct communication were detected.

Case 5

Iron Deposition in the Liver

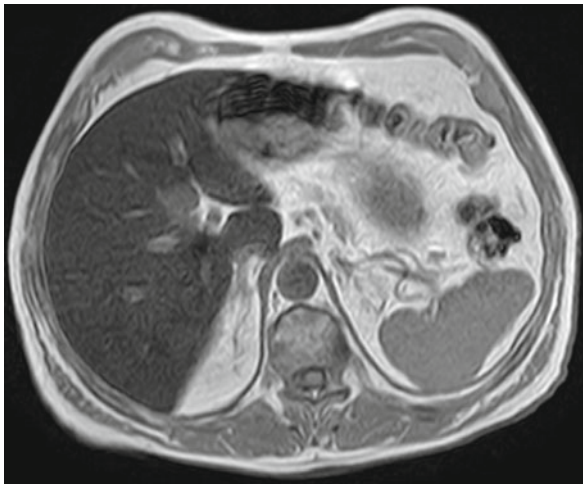

Fig. 1.5.1

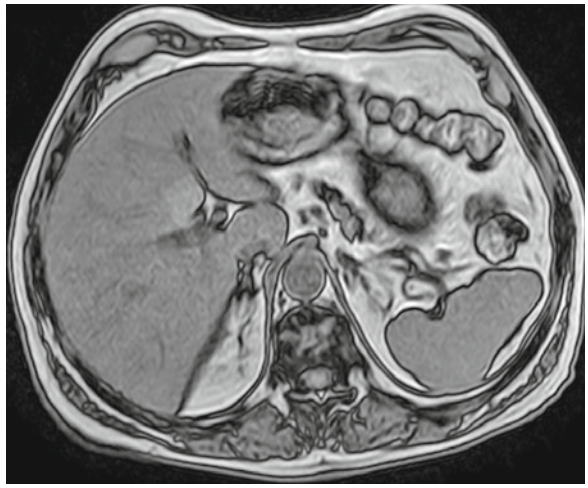

Fig. 1.5.2

Fig. 1.5.3

Clinical Information

A 32-year-old man, who complains of arthralgias, fatigue, and decreased libido, revealed hyperpigmentation of the skin on physical examination. The blood test drawn detected an increased transferrin saturation, high ferritin values, and slight increase in LFTs. With the suspicion of hemochromatosis, an MRI scan was requested. The protocol includes chemical shift and multi-echo T2-weighted images.

Comments

Iron can accumulate in the liver in the clinical setting of either primary or secondary hemochromatosis.

Primary hemochromatosis, idiopathic or genetic, is a common hereditary disorder secondary to a genetic mutation that determines an excessive gastrointestinal iron absorption with a consequent increase in tissue deposits: liver, heart, pancreas, pituitary, joints, and skin, among others. Without treatment, it produces organ damage and, in the liver, develops cirrhosis, and even a hepatocellular carcinoma could appear. Iron and hemosiderin accumulate in hepatocytes and induce cell damage with the development of fibrous septa and a micronodular cirrhosis. There is no significant accumulation of iron in the biliary epithelium or in the reticuloendothelial system. The detection of iron in the pancreatic parenchyma correlates with irreversible changes associated to cirrhosis.

Transfusional iron overload is the most common cause of increased iron storage in the liver and secondary hemochromatosis. Cirrhosis is rare, and iron deposition occurs predominantly in the reticuloendothelial system. The spleen is affected, and the pancreas is spared.

In hemolytic anemia, the findings of primary and secondary hemochromatosis coexist, as there is an increased iron absorption and a history of multiple transfusions. Cirrhosis also causes increased cellular levels of iron in the liver, by a mechanism that is not well understood.

In unenhanced CT scans, liver density is uniformly elevated, between 75 and 135 HU (normal values are below 65 HU).

MRI is probably the noninvasive technique of choice for the determination of hepatic iron. Increased levels of iron in the liver can be detected in MRI based on magnetic susceptibility artifact. The most effective sequences to detect such artifacts are gradient-echo T2-weighted sequences. There is a direct correlation between the liver signal to muscle intensity ratio and the amount of hepatic iron. Multiecho T2 sequences with assessment of liver parenchyma signal decay allow an accurate quantification of iron deposits, and it is a useful tool for posttreatment monitorization.

Chemical-shift imaging is also a standard part of the liver MRI scan protocols. Characteristically, the increase in hepatic iron deposits produces a liver signal drop in GE T1-weighted in-phase sequences with respect to out-of-phase ones. This is explained because the echo time in in-phase is longer than in out-of-phase, and the magnetic susceptibility produced by the iron excess is detected.

Imaging Findings

In-phase GE T1-weighted image (Fig. 1.5.1) shows a marked reduction in liver parenchyma signal, more evident when the in-phase acquisition is compared with the out-of-phase GE T1-weighted image (Fig. 1.5.2). The T2-weighted sequence (Fig. 1.5.3) identifies the liver with a lower intensity than that of the paraspinal muscles. The iron deposit estimation with a gradient-echo T2-weighted sequences with different TE was 200 μmol/g in this case (not shown), which is in the limit between moderate and major overload.

Case 6
Liver Cirrhosis

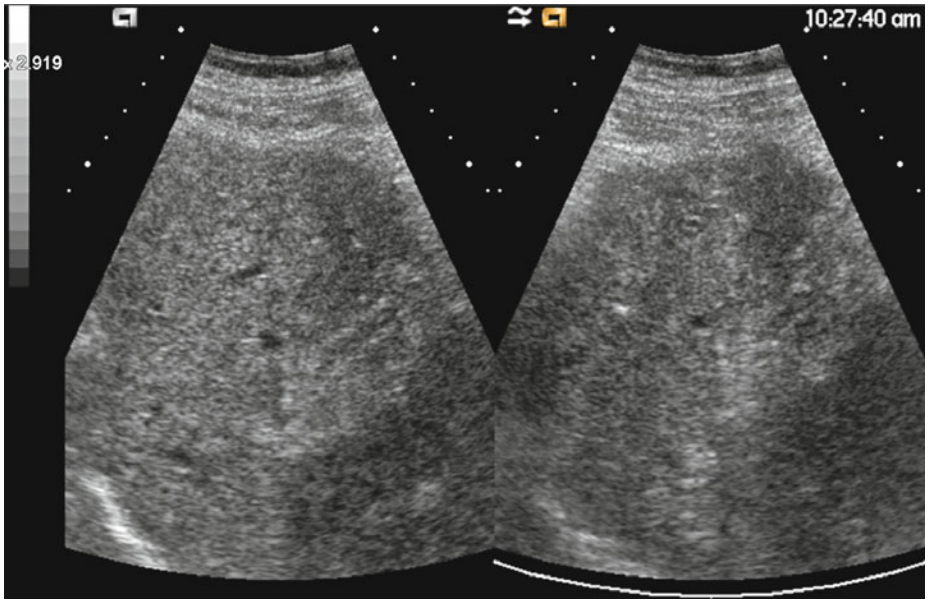

Fig. 1.6.1

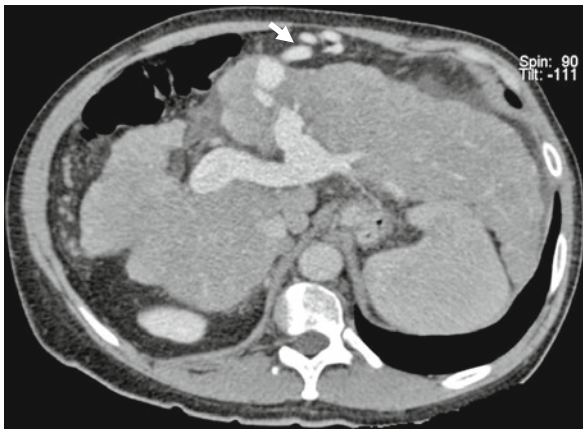

Fig. 1.6.2

Fig. 1.6.3

Clinical Information

A 53-year-old male with personal history of hepatitis C virus infection. He did not receive any specific treatment. Physical examination identified increased abdominal girth, with ascites, periumbilical centrifugal superficial venous circulation, and splenomegaly. Blood test drawn showed altered LFTs, high ammonium, mild hyperbilirubinemia, and hypoalbuminemia. Ultrasound is requested for suspected chronic liver disease, with probable cirrhosis and portal hypertension.

Comments

Liver cirrhosis is a chronic disease characterized by parenchymal extensive fibrosis and architectural distortion by regenerative liver nodules. Cirrhosis prevalence in autopsy series has been estimated between 5% and 10%. The most common causes of cirrhosis include hepatitis C virus (55% of cases), hepatitis B (16%), alcoholism (13%), and other causes, such as nonalcoholic steatohepatitis (NASH) and biliary cirrhosis. Morphologically, cirrhosis can be classified in macronodular (alcoholism), micronodular (hepatitis B), or mixed (bile duct obstruction). The diagnosis of cirrhosis has been traditionally established by liver biopsy but can often be suggested by imaging findings. Portal hypertension is commonly associated to advanced cirrhosis. It is due to increased elevated pressure despite formation of portal collateral vessels.

Generally, the monitorization of patients with cirrhosis is done with ultrasound; CT and MRI studies are performed, when a nodular lesion is detected or when there is an alteration of the hepatic architecture.

The key factors in imaging studies are a nodular contour, widened fissures, enlargement of segment 1 or caudate lobe, ascites, splenomegaly, and portacaval shunts, as signs of portal hypertension. There are other causes of segment 1 hypertrophy, not associated with cirrhosis, as is seen in sclerosing cholangitis and Budd-Chiari disease. The morphological changes in the metastatic liver, which occur in response to chemotherapy, may mimic cirrhosis.

In patients with cirrhosis, a relatively common finding in enhanced CT or MRI studies is the existence of arteriovenous shunts and regional disturbances of hepatic perfusion that sometimes simulate hypervascular nodules. Splenic siderotic nodules can also be detected (Gamna-Gandy bodies) as a sign of portal hypertension. These nodules are seen primarily on MRI scans with GE T2-weighted sequences that show a higher magnetic susceptibility between all the rest of common sequences of a liver MRI protocol.

Cirrhosis is a predisposing factor for portal vein thrombosis and is essential to make the distinction between neoplastic and benign thrombus. Demonstration of vessels within the thrombi or enhancement of the thrombus is a diagnostic sign of malignant thrombosis.

Imaging Findings

Figure 1.6.1 Abdominal ultrasound showed an enlargement of liver segments 2 and 3 and atrophy of segment 4 and right lobe. The liver contour is nodular, and its echotexture is altered. The caliber of the hepatic veins is reduced.

It was decided to perform a CT because the liver echotexture disturbances can hide nodular lesions. We performed a CT protocol that consists of 3 phases: late arterial liver

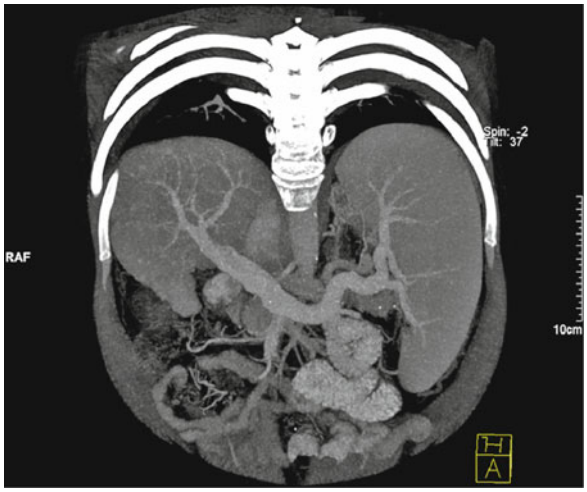

Fig. 1.6.4

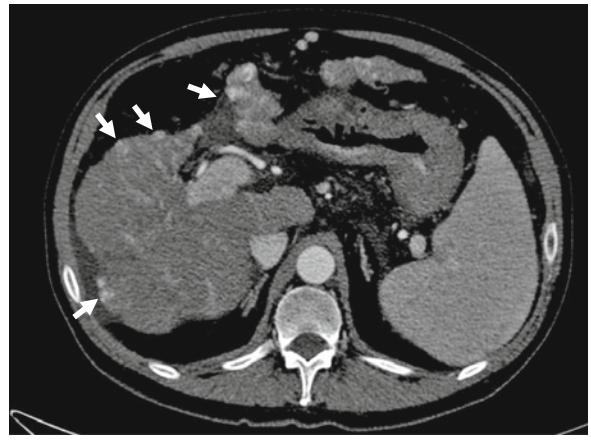

Fig. 1.6.5

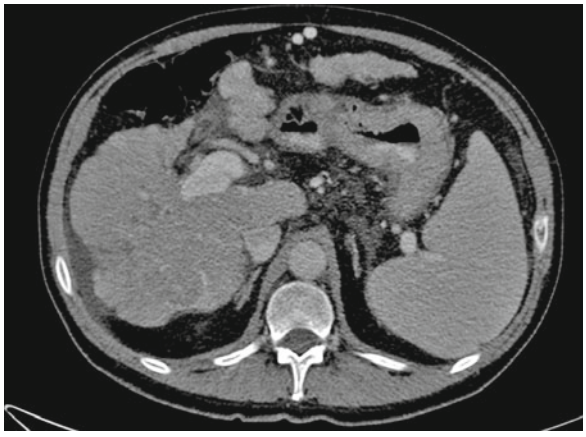

Fig. 1.6.6

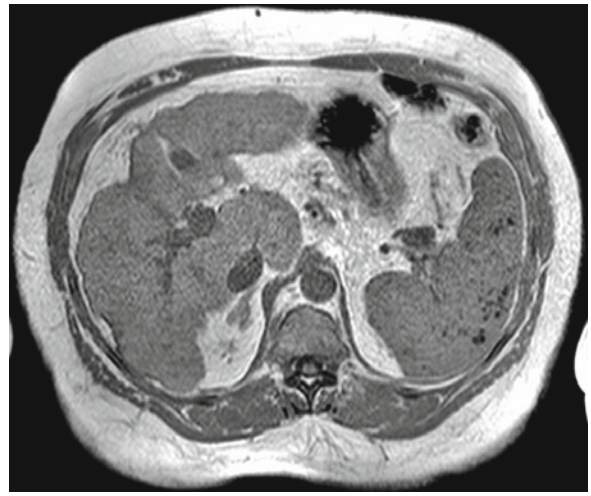

Fig. 1.6.7

(6 s delay after aortic arterial enhancement above 200 HU, using bolus detection technique), portal phase at 70 s, and a late or equilibrium phase (180 s after the start of contrast media injection). The contrast dose is 2 mL/kg of body weight, and a powered injector was used. The CT findings confirmed the altered liver morphology, demonstrating atrophy with capsular retraction of segment 4 (Fig. 1.6.2, enhanced CT on the portal phase). Paraumbilical venous system recanalization was confirmed (*arrows* on Figs. 1.6.2 and 1.6.3) (Fig. 1.6.3, volume rendering of CT on portal phase). There was an important splenomegaly, and the portal vein diameter was increased (Fig. 1.6.4, oblique coronal MPR of enhanced CT on portal venous phase). Multiple arteriovenous anomalous communications (*arrows* on 1.6.5) were demonstrated (Figs. 1.6.5 and 1.6.6, enhanced CT on the arterial and venous phases, respectively). Splenic Gamna-Gandy bodies were also demonstrated in an MRI study (Fig. 1.6.7, in-phase GE T1-weighted sequence).

Case 7

Hepatic Pseudolesion: Focal Fatty Area

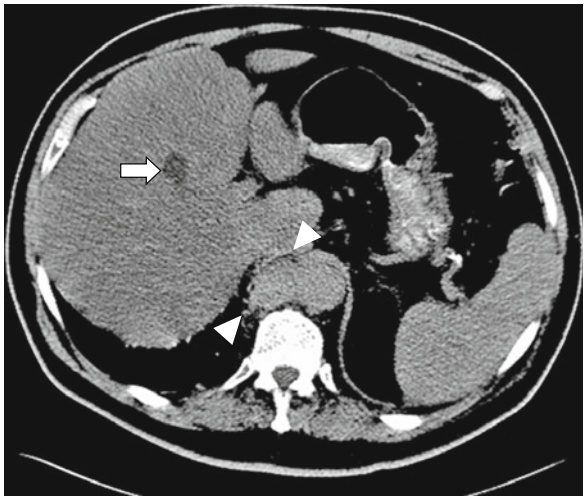

Fig. 1.7.1

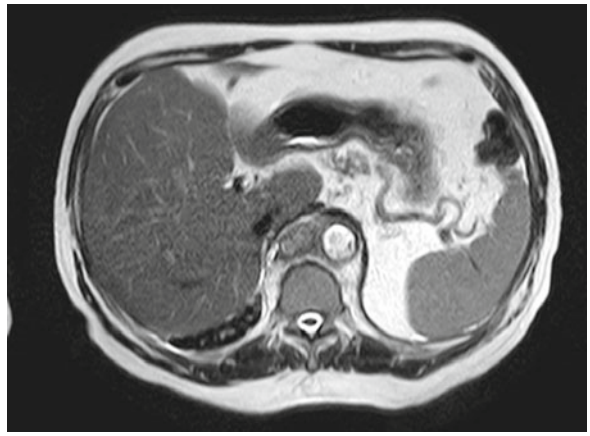

Fig. 1.7.2

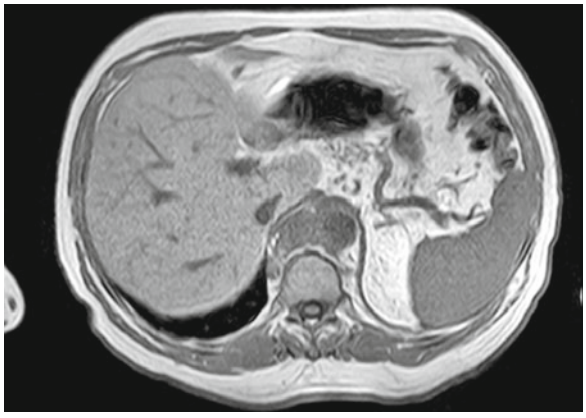

Fig. 1.7.3

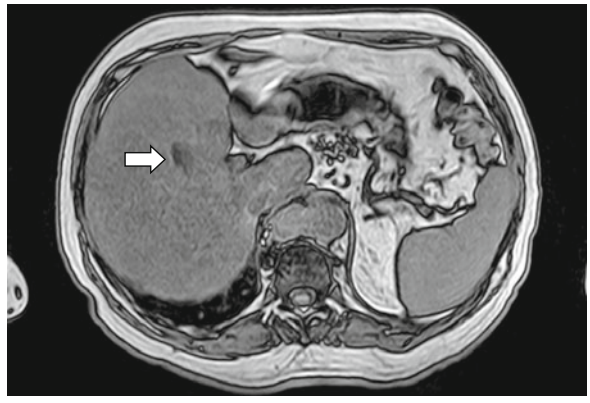

Fig. 1.7.4